

Originally published as:

Hagg, W., Braun, L. N., Weber, M., Becht, M., 2006. Runoff modelling in glacierized Central Asian catchments for present-day and future climate. *Nordic Hydrology* 37/2: 93-105.

Runoff modelling in glacierized Central Asian catchments for present-day and future climate

W. Hagg¹, L.N. Braun¹, M. Weber¹ and M. Becht²

¹Commission for Glaciology, Bavarian Academy of Sciences, Marstallplatz 8, 80539 Munich, Germany.

E-mail: wilfried.hagg@lrz.badw-muenchen.de

²Faculty of Mathematics and Geography, Catholic University Eichstätt-Ingolstadt, Ostenstrasse 18, 85072 Eichstätt, Germany.

Received 10 November 2004; accepted in revised form 22 September 2005

Abstract A conceptual precipitation–runoff model was applied in five glacierized catchments in Central Asia. The model, which was first developed and applied in the Alps, works on a daily time step and yields good results in the more continental climate of the Tien Shan mountains for present-day climate conditions. Runoff scenarios for different climates (doubling of CO₂) and glacierization conditions predict an increased flood risk as a first stage and a more complex picture after a complete glacier loss: a higher discharge during spring due to an earlier and more intense snowmelt is followed by a water deficiency in hot and dry summer periods. This unfavourable seasonal redistribution of the water supply has dramatic consequences for the Central Asian lowlands, which depend to a high degree on the glacier melt water for irrigation and already nowadays suffer from water shortages.

Keywords Central Asia; climate change; glacier hydrology; runoff modelling

Introduction

The retreat of mountain glaciers is a worldwide observed phenomenon. One of the causes can be found in the rise of air temperature, which turns glaciers into important indicators for global warming, while the primary impact lies in runoff changes of glacier-fed rivers. Although some remarkable research efforts have been made, the interrelations between climate, glaciers and discharge are not yet completely understood. To enable a global view on this topic, it is essential to collect results from different climatic regions. Central Asia possesses areas with vast glaciation and is characterized by a continental climate that differs greatly from other mid-latitude mountain regions. Therefore, and because of the enormous importance of glaciers for the water supply of dry lowlands, high mountains in Central Asia are an especially interesting region for catchment hydrology studies.

The aim of this work is to estimate the effect of glacier retreat on water yield from high mountain areas of Central Asia by applying a conceptual precipitation–runoff model at several test sites. Because of its robust performance and its low demands on input data, the HBV-ETH model was chosen for this purpose. The model is capable of calculating water balance components on a daily timestep for current and for modified climate and glacierization conditions.

Description of research areas

Studies have been carried out at five test sites located in different parts of the Tien Shan Mountains. These are Tuyuksu Glacier in Kazakhstan, Abramov Glacier and Ala Archa basin in Kyrgyzstan, Oigaing basin in Uzbekistan and Glacier No. 1 in China (Figure 1).

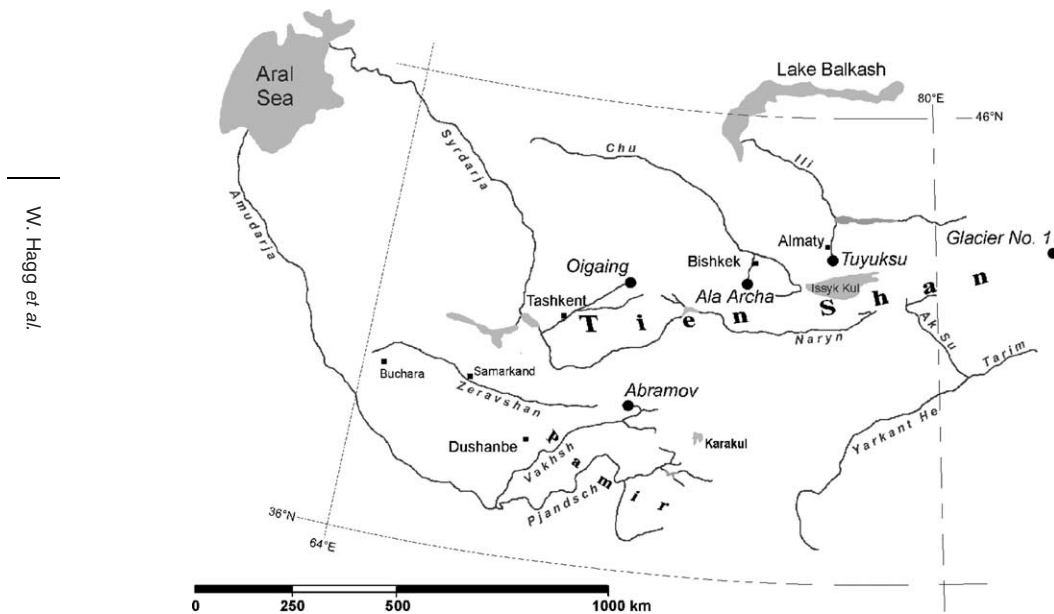


Figure 1 Location of test sites

The Tuyuksu area is located on the northern slope of the Zailiskiy Range, which is the most humid part of the northern Tien Shan. Annual precipitation is around 1000 mm, with a maximum in late spring or early summer. The basin is drained by the Little Almatinka River, which feeds the Ili River ending in Lake Balkash. The catchment area at the gauging station is 28 km², with a total glaciation of 7 km². The largest of the nine glaciers is Central Tuyuksu with an area of 2.5 km² and an altitudinal range from 3415 m to 4219 m a.s.l. ([Kommission für Glaziologie 2003](#)).

The basin of the Ala Archa River is situated in the Kyrgyz Range, west of the Tuyuksu area, and belongs to the catchment of the Chu River, which dries up in the Kazakh lowlands. Precipitation reaches 700 mm per year and has its maximum in spring ([CADB 2003](#)). The basin area is 31 km², 36% of which is covered with glaciers, which reach from 4100 m a.s.l. down to 3400 m a.s.l.

The Oigaing basin in the northwestern Tien Shan belongs to the drainage area of the Sirdarya River, one of the main inflows of the Aral Sea. With a total area of 463 km² and a glacier area of 42.5 km² this basin represents a larger and a less glacierized (7%) example. The catchment lies between 2140 m a.s.l. and 4300 m a.s.l., while the glaciers reach down to 3400 m a.s.l. At an altitude of 2140 m a.s.l., annual precipitation is 720 mm with a summer maximum ([CADB 2003](#)).

The Abramov Glacier is located in the Pamiro-Alay, a transition zone between Tien Shan and Pamirs. The area is less exposed to Atlantic air masses and has an annual precipitation of slightly above 700 mm, most of which falls in spring. The melt water feeds the Koksou River, a third degree tributary of the Amudarya River. The basin has an area of 58 km², with a glaciation of 51%. There are 10 small glaciers and the Abramov glacier with an area of 26 km² ([WGMS 1999](#)), that stretches from 3625 to 4960 m a.s.l. and is mostly oriented northwards.

Glacier No. 1 is situated in the extremely continental, eastern part of the Tien Shan. From the source area of the Urumqi River, it supplies the city of Urumqi and large agricultural areas with water before the river dries up in the desert. Annual precipitation on the glacier is only about 400 mm, and because of the strong influence of the Siberian High in winter, it is

concentrated in the summer months. Therefore, accumulation and ablation take part simultaneously in different elevation belts and both reach their maximum in summer (“summer accumulation glacier type”, after [Ageta and Higuchi \(1984\)](#)). The watershed of the hydrometric station is 3.34 km², with a glaciated area of 1.9 km², which is located at altitudes between 3700 and 4486 m a.s.l. ([WGMS 2001](#)).

Model description

The conceptual precipitation–runoff model HBV was developed in the 1970s in Sweden ([Bergström 1976](#)) and expanded at the Swiss Federal Institute of Technology (ETH) in Zurich for application in glacierized regions ([Braun and Renner 1992](#)). Further improvements and the programming for operational use on microcomputers were carried out in 1997 at the Commission for Glaciology of the Bavarian Academy of Sciences ([Braun et al. 2000](#)). [Figure 2](#) shows the structure of the current version of the HBV-ETH model, while [Table 1](#) lists the calibration parameters.

As input, the model needs distribution of the basin area by altitude and topographic aspect, where the glaciated parts have to be treated separately. For running the model, the only required data are daily means of air temperature and precipitation. Daily runoff is needed for calibration; an additional quality check can be performed by comparing calculated glacier mass balance with measured values.

The snow and glacier subroutine calculates melt rates of the snow and ice cover distributed in different elevation belts and aspect classes; the further steps of the model are performed on a lumped basis for the whole catchment area. Aggregational state and amount of precipitation is determined for each elevation belt with a threshold air temperature (T_0) and a constant lapse rate for temperature (TGRAD) and precipitation (PGRAD). Correction factors for rain and snow (RCF and SCF) account for errors in precipitation measurement and for the representativeness of the weather station for the catchment. Melting of snow and ice is calculated with the degree day approach using a seasonally variable degree day factor,

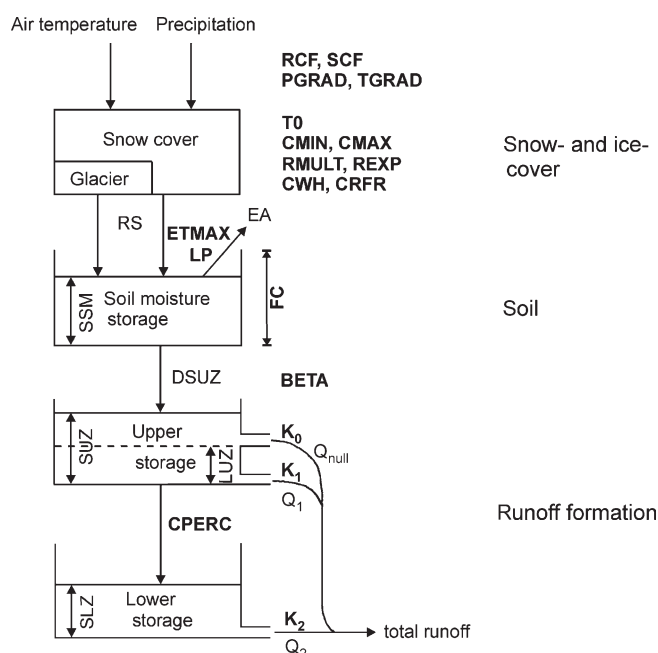


Figure 2 Schematic representation of the HBV-ETH model (based on [Bergström 1976](#)). Parameters that need to be optimized are in bold

Table 1 Description of the free parameters in the HBV-ETH model

Parameter	Description	Unit
RCF	Rainfall correction factor	–
SCF	Snowfall correction factor	–
PGRAD	Precipitation gradient	%/100 m
TGRAD	Temperature gradient	°C/100 m
T0	Temperature divider (also general temperature correction)	–
CMIN	Minimum degree day factor on 21 December	mm °C ⁻¹ d
CMAX	Maximum degree day factor on 21 June	mm °C ⁻¹ d
RMULT	Multiplicative factor to account for ice melt	–
REXP	Multiplicative factor to account for topographic aspect	–
CWH	Water holding capacity of snow	–
CRFR	Coefficient of refreezing	–
ETMAX	Maximum evapotranspiration on 1 August	mm/d
LP	Limit for potential evapotranspiration	mm
FC	Field capacity	mm
BETA	Coefficient to calculate outflow of soil moisture storage	–
CPERC	Percolation from upper to lower storage	mm/d
k_0, k_1, k_2	Storage discharge constants	–

assuming a maximum (CMAX) and a minimum (CMIN) value at the summer and winter solstice, respectively. To take into account the varying radiation input in alpine terrain, computation of melt rates is corrected for aspect. On south facing slopes melt is multiplied by the factor REXP (> 1) while on north facing slopes it is divided by the same value. Enhanced melt of ice as compared to snow due to the lower albedo is considered by the multiplicative factor RMULT (> 1). The storage of liquid water in the snow pack (CWH) is included as well and refreezing of water in the snowpack can be calculated with a coefficient (CRFR). Glacier mass balance is determined for each elevation and aspect unit.

The sum of rainfall and meltwater output (RS) is then transferred to the soil moisture routine, a reservoir from where actual evapotranspiration (EA) is calculated as a function of potential evaporation and soil moisture storage (SSM). The portion of the water which does not evaporate gets into the upper storage. This inflow (DSUZ) is calculated by RS, SSM, the field capacity (FC) and a coefficient (BETA).

In the last model component, consisting of an upper (SUZ) and a lower storage (SLZ), the remaining water is transformed into the flow hydrograph. Three outflows with different response times ($Q_{\text{null}}, Q_1, Q_2$) are calculated by constants (k_0, k_1, k_2). Quick runoff (Q_{null}) only appears if the fill level of the upper storage (SUZ) exceeds a certain value (LUZ). Percolation from the upper to the lower storage (groundwater storage) is controlled by the constant CPERC. At the end, the three outflows are summed to yield total runoff in a daily time step.

The calibration of the model parameters is done by a manual optimization procedure, where the simulated hydrograph is compared with measured discharge. This is somewhat tricky, because errors in ice melt rates can be compensated by erroneous basin precipitation (see, for example, Braun and Aellen 1990). To avoid this kind of error compensation, it is helpful to compare calculated glacier mass balances with data observed in the field.

Melting of permafrost and dead ice bodies are additional sources of runoff. However, these are not accounted for by the HBV-ETH model. It is believed that they play only a minor role in quantitative hydrological observations. Soil characteristics dependent on permafrost, such as field capacity and percolation rates, are considered as a whole when calibrating model parameters.

Modelling results for present-day climate

Goodness of fit

Figure 3 shows observed and calculated hydrographs for one example year in each test area.

Numerical parameters for the goodness of fit (Table 2) show satisfactory values. Especially in the Abramov region, the model efficiency criterion following Nash and Sutcliffe (1970) indicates good results. At this test site the data series is long enough to separate a calibration period, for which the parameter values are optimized, from a validation period, in which this parameter set is tested.

Worldwide testing of conceptual models (Rango 1992) has shown that R^2 values higher than 0.8 are above average for runoff modelling in glaciated catchments. Generally, comparison of R^2 values between different basins has to be regarded carefully, because this statistical item is strongly influenced by runoff variability, which may explain the relatively low values at Glacier No. 1, where runoff variability is highest, due to the small size of the catchment and the absence of a ground body that can act like a buffer.

At Tuyuksu, Abramov and Glacier No. 1, measured glacier mass balances served as an additional quality check. For this purpose, the model delivers curves for calculated net balances versus altitude and exposition which are evaluated graphically against measured point values. Plausible results were obtained in all three catchments.

Hydrological balance

Mean annual terms of the water balance in the five investigation areas as calculated by the HBV-ETH model are shown in Table 3.

The most striking fact is the slightly positive mean annual glacier mass balance at Oigaing. There are no mass balance measurements available for comparison in this area, but Severtsova glacier in the Oigaing catchment shows front variations from 1976–1980 of -0.9 m (Fluctuations of Glaciers Vol. IV), including two years of glacier advance ($+10$ m in 1977 and $+17.6$ m in 1978). This indicates that the glaciers could have been in a stable state during the observed period.

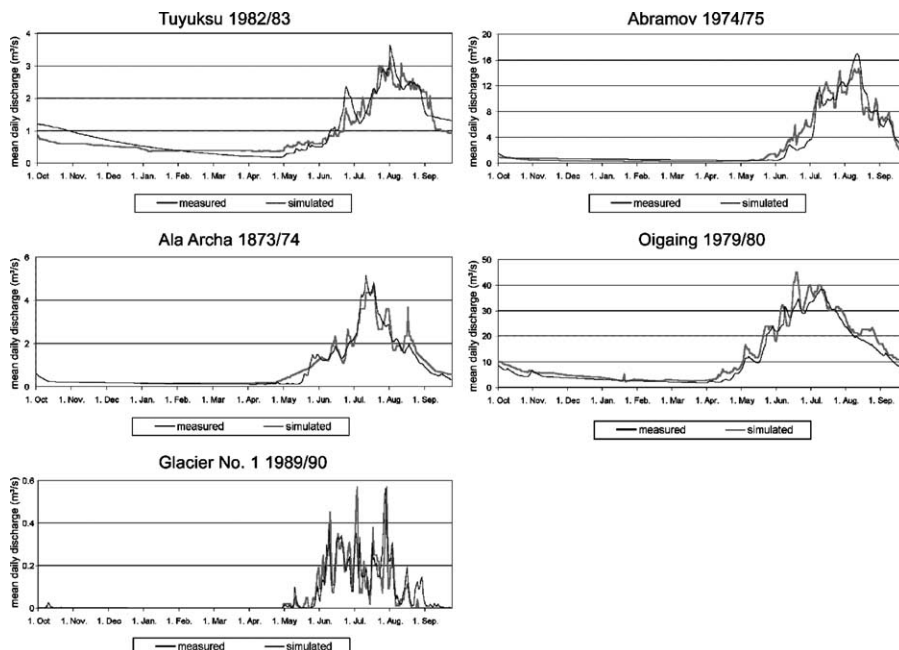


Figure 3 Comparison between measured and simulated daily discharge for one example year in each test area

Table 2 Goodness of fit for the five investigation areas (Q_{diff} = accumulated difference between measured and simulated discharge in mm/a (percentage of the measured value), R^2 = Nash–Sutcliffe criterion)

	$Q_{diff,mean}$	$Q_{diff,min}$	$Q_{diff,max}$	R^2_{mean}	R^2_{min}	R^2_{max}
Tuyuksu (1981/82–1984/85)	77 [7.6%]	10 [1.0%]	185 [18.3%]	0.81	0.80	0.85
Ala Archa (1960/61, 1962/63–1963/64, 1971/72–1972/73)	127 [13%]	8 [1.0%]	398 [30.2%]	0.88	0.80	0.94
Oigaing (1971/72–1972/73, 1978/79–1979/80)	66 [7.8%]	24 [2.8%]	113 [11.1%]	0.89	0.77	0.96
Abramov (1968/69–1977/78) calibration period	226 [14.5%]	117 [8.3%]	539 [25.0%]	0.85	0.77	0.91
Abramov (1979/80–1987/88) validation period	283 [16.7%]	30 [2.7%]	566 [35.9%]	0.83	0.70	0.91
Glacier No. 1 (1986/87–1989/90)	113 [21.1%]	31 [7.8%]	191 [31.6%]	0.76	0.73	0.78

Runoff scenarios for future climate

Modification of input data

Climate scenario outputs for the doubling of CO_2 were taken from Kazakhstan Climate Change Study (KazNIIMOSK 1999), where climate modelling was carried out for the Tuyuksu region by applying the following Global Circulation Models (GCMs): GFDL and GFDL-T (Geophysical Fluid Dynamics Laboratory, University of Princeton), UKMO (Meteorological Agency of the UK), CCC (Canadian Climate Center) and GISS (Goddard Institute for Space Studies). All models take into account CO_2 concentration only, but not aerosol variations. Regional climate change scenarios were prepared by statistical downscaling techniques. Three time series of global air temperature anomalies were used to develop relationships with the local climate, which reached correlation coefficients between 0.3 and 0.5 (KazNIIMOSK 1999). As a next step, linear regression parameters between global temperature anomalies and the mean annual (and seasonal) anomalies at the meteorological stations were calculated. Results of the regional scenarios show a range of possible temperature increases between 3.7°C (GFDL) and 7.1°C (CCC). Precipitation changes are less conclusive and, according to most models, a slight increase is expected. Since the GISS model showed the best agreement with measured temperatures in the $1 \times CO_2$ model runs (KazNIIMOSK 1999), its output was chosen to serve as a template for the HBV model input.

To create these input files, the mean monthly changes of the GISS predictions had to be incorporated into the daily data set to drive the HBV model. In principle, it is possible to generate climate data stochastically using weather generators (Richardson 1981; Semenov et al. 1998), but in practice, the results will be strongly influenced by the capability of the individual stochastic model to reproduce temporal patterns realistically (IPCC 2001). Moreover, the application of synthetic weather data in areas with sparse data is difficult in

Table 3 Annual terms of the water balance as determined by the HBV-ETH-model (Q = runoff, P = basin precipitation, ET = basin evapotranspiration, S = storage changes) in mm/a

	Q	P	ET	$S_{glacier}$	S_{snow}	S_{ground}
Tuyuksu (1958/59–1997/98)	943	982	146	–131	19	5
Ala Archa (1960/61–1964/65, 1971/72–1973/74)	845	636	151	–382	12	10
Oigaing (1962/63–1964/65, 1971/72–1973/74, 1978/79–1979/80)	778	997	148	10	55	5
Abramov (1968/69–1987/88)	1348	1146	167	–460	57	34
Glacier No. 1 (1986/87–1989/90)	443	551	231	–135	39	–27

regions with heterogeneous climate such as high mountain test sites. Since a data set of only a few years had to be created and because of the mentioned limitations of more sophisticated methods, the temporal downscaling was done manually by adding hot days and introducing or deleting precipitation events so that the anticipated monthly changes were achieved. To avoid discussing particularities of one individual year, two reference years with differing meteorological conditions and glacier mass balances were chosen. This procedure requires meteorological knowledge and sensibility of the modeler, but leads to a more realistic description of weather conditions after a climate change than a general temperature shift (Escher-Vetter *et al.* 1999).

Little is known about future evapotranspiration changes. In a warmer atmosphere, potential evapotranspiration will increase, but it is not clear how actual evapotranspiration will behave. The actual rate of evaporation is constrained by water availability and could, for example, be reduced by a shortage of soil water in summer (IPCC 2001). According to some authors, global warming will concentrate future precipitation in heavy rainfalls (Hennessy *et al.* 1997; McGuffie *et al.* 1999) and consequently dry periods between these events will be extended (e.g. Schädler, pers. comm.). Such changes in the precipitation pattern and soil moisture content could lead to a decrease of actual evapotranspiration. Since evapotranspiration plays a minor role in the water balance of high alpine catchments and due to better knowledge of future changes, its value was not modified in the runoff scenarios.

Results

The effect of climate change on river streamflow was simulated for the current glacier extent and for two stages of deglaciation: after an areal reduction by 50% (elimination of the lower half of the glacierized area) and after complete melting.

Figure 4 shows the hydrographs of the reference years and the $2 \times \text{CO}_2$ scenarios. Some similarities can be observed in nearly all cases:

Coupling a doubling of CO_2 with current glaciation, discharge begins earlier in the year and rises towards summer, increasing the flood risk. This case has to be regarded as hypothetical and it displays only a trend, because a current glacier extent is hardly realistic after such a climate change, but is expected to be much smaller.

If the glacierized area is reduced by 50%, snowmelt still begins one month earlier and is more intense, but the summer peaks are mostly reduced to the same level that was already observed in the reference year.

The complete disappearance of glaciers yields a water shortage in summer. River hydrograph is controlled by groundwater release and rainfall events only and takes on very low values during dry periods. An increase of runoff during snowmelt can still be observed.

In the Oigaing river basin, deglaciation has no effect on streamflow for the reference year with little glacier melt and only little effect for the warmer reference year. At this test site, hydrographs for the different steps of glacier retreat are more or less identical. The catchment reaches down to lower elevations and is less glaciated (7%) than the others, which explains the nivo-pluvial runoff regime.

Figure 5 shows the monthly hydrological responses after climate warming and areal reduction, related to the two reference years.

Reduction of glaciated area by 50%

The higher frequency of peaks increases monthly runoff in summer. This means that the glaciers produce more melt than in the reference years, although they lost half of their area. This seems surprising at first glance, but can be explained by the rise of the equilibrium line altitude (ELA) which leads to icemelt in higher elevation zones. The most productive part of a glacier in respect to melt water yield is the ablation area below the firm line. The area of this

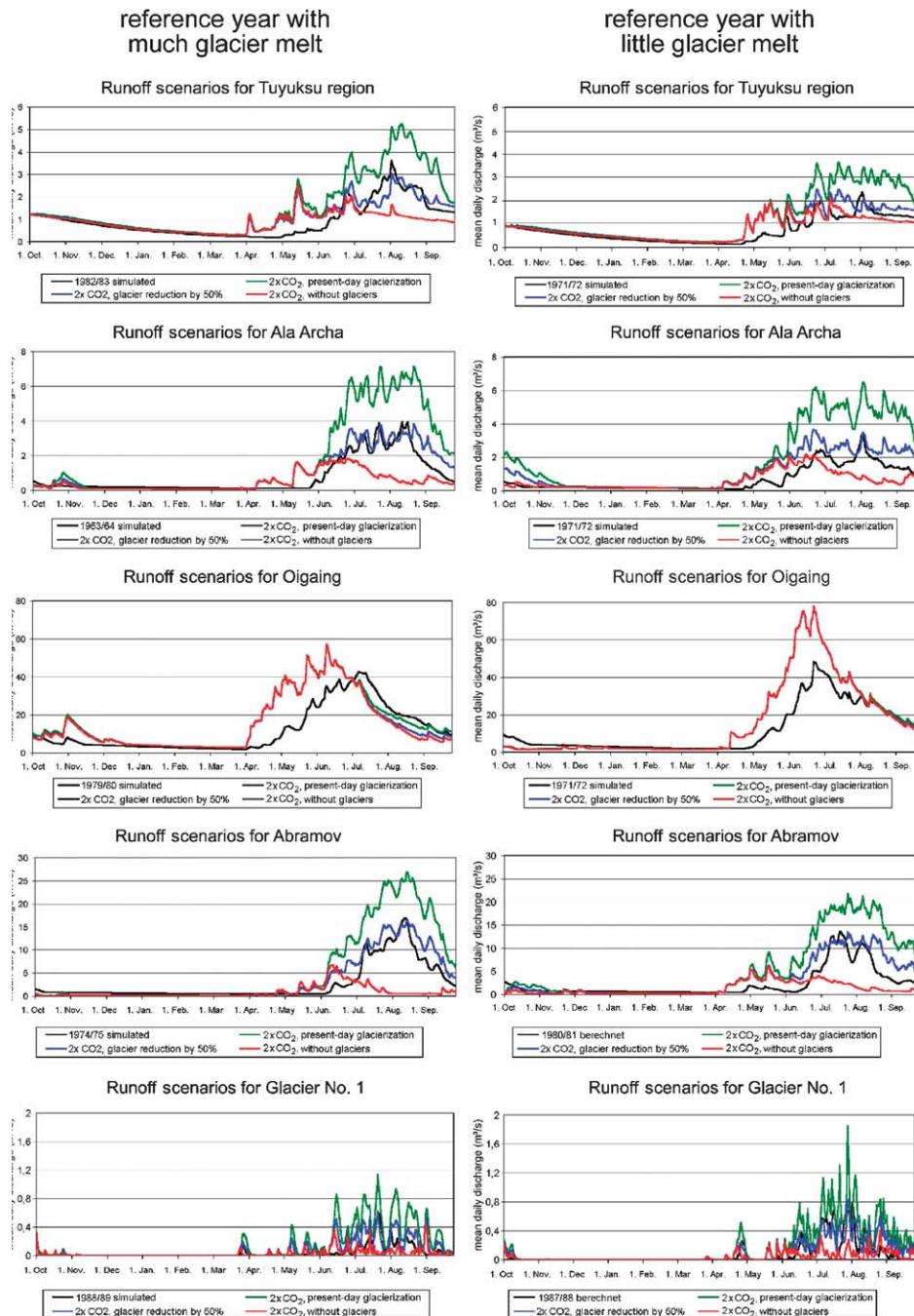


Figure 4 Calculated daily discharge of the reference year and of a climate scenario after the doubling of CO₂ (predicted by the GISS model), for three different steps of deglaciation

bare ice zone with lower albedo is determined not only by the total area of the glacier, but also by the accumulation area ratio (AAR). A reduction of the glacier area by 50% does not necessarily mean a similar reduction of the bare ice zone: the ablation area can, in the same manner, stay equal or in some cases even increase, especially when ELA was very low in the reference period.

Volumetric difference in monthly runoff (related to summer runoff of the reference year) after reduction of glaciated area by 50% after complete melting of glaciers

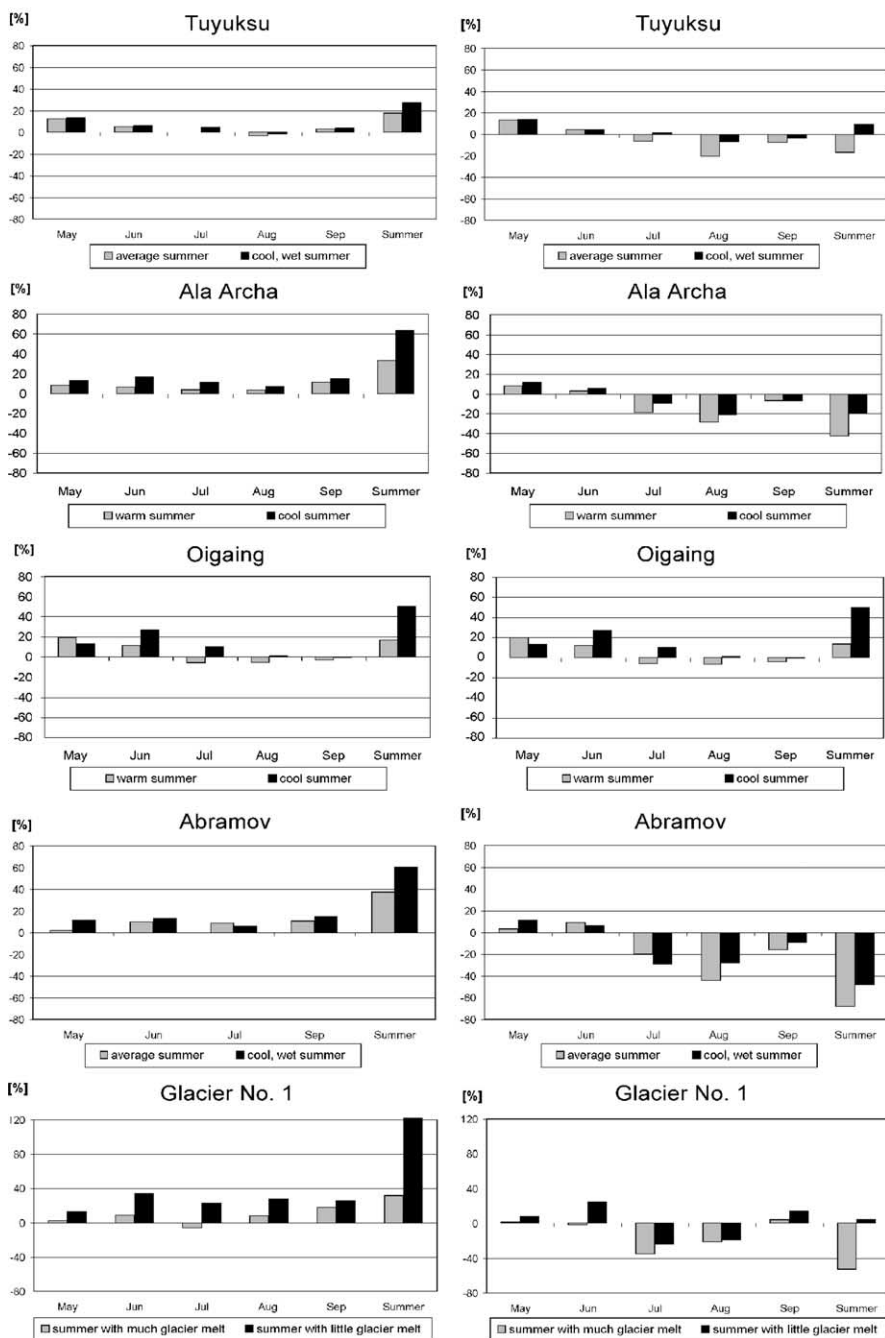


Figure 5 Effect of climate change (predicted by the GISS model for the doubling of CO₂) and glacier degradation on monthly discharge, related to summer runoff of the two reference years

The scenarios show a higher increase in runoff for the cooler reference year than for the warmer one, where glacier melt and discharge were already high before the assumed climate warming. In the Tuyuksu region, the relatively small water yield can only be explained with the low glaciation (12.5%) in combination with high groundwater infiltration in the relatively

flat areas between 3000 and 3100 m a.s.l. This catchment possesses a huge moraine body below the continuous permafrost zone that acts like a buffer and weakens the hydrological reaction. The basin of Glacier No. 1 shows a strong response to climate warming for the reference year with little ice melt.

Complete melting of glaciers

The qualitative changes in monthly runoff due to a complete disappearance of glaciers are quite similar in all investigation areas. However, there are quantitative differences (Figure 5). Noticeable changes begin in May or June, where all sites show an increase in runoff as a consequence of a more intense snowmelt up to higher elevations. In the main ablation season, the absence of glacier melt leads to a remarkable reduction of discharge. In contrast to the above described scenarios, the strongest effect is achieved for the hotter reference years with a more intense glacier melt. Monthly runoff decreases from July to September in most of the cases, but in the cooler reference years, this effect can be compensated by the enhanced snowmelt in spring, so that total runoff from May to September increases at Tuyuksu and Glacier No. 1. The Oigaing basin is again an exception; here the climatological impact on snowmelt has much bigger consequences than the areal shrinkage of the small glacier cover and river streamflow increases in spring, but almost remains unchanged in summer. The hydrological impact of glaciers is weak in this catchment and monthly changes in runoff show almost the same values as for current glaciation, for glacier reduction by 50% and for complete disappearance.

The effect of glacier degradation on runoff is mainly controlled by the contribution of glacier melt to the total discharge of the reference year, and this contribution is again strongly influenced by the degree of glaciation, by glacier mass balance and by typical seasonal weather patterns. Table 4 shows the reduction of discharge due to the disappearance of glaciers, the percentage of glacial meltwater to total discharge and the factors controlling this portion.

In the Tuyuksu region, the rather slight hydrological response to glacier disappearance can be explained by the low degree of glaciation (25%) and by the fact that two cool reference years had to be chosen, due to problems with the quality of data. Moreover, the hydrograph is smoothed by the huge groundwater reservoir above the gauging station, which is filled in spring and drained during summer (Makarevich, pers. comm.).

At the Oigaing basin, the summers are very dry, but the small glaciation (7%) and the balanced mass behaviour of the glaciers lead to a low percentage of glacier melt in total runoff.

The strongest reduction of discharge occurs at the Abramov glacier. The summers in this highly glacierized (55%) region are typically dry, mass balances are negative and therefore the contribution of glacial meltwater to total runoff is very large.

The hydrological effect is also very high at Glacier No. 1, even in the year with a balanced glacier mass budget. Maybe this test site is not comparable to the others because of its small size. The model gives best results if no percolation into groundwater storage is assumed. This seems realistic with regard to the high elevation, as the whole catchment area is located within the permafrost zone. Without glaciers, runoff only occurs after precipitation and with this set of model parameters no baseflow can be generated and discharge almost drops to zero on days with no melt conditions.

It can be outlined that in most cases the intensity of the hydrological reaction after a climate warming and complete glacier loss can be explained by the glaciation of the catchment and the mass balance of the reference year.

Table 4 Hydrometeorological conditions of the reference years and change in discharge in the main ablation season after doubling of CO₂ and complete melting of glaciers as calculated by the HBV-ETH model

Catchment area (glaciation)	Year	Weather conditions (Jul–Aug)		Percentage of glacier melt (Jul–Aug) in total runoff (%) (longterm mean)	Glacier mass balance, related to catchment area (mm)	Change of discharge in July–August (%) (related to summer runoff)	Runoff coefficient (longterm mean)
		Extrapolated temperature at mean glacier elevation (°C) (longterm mean)	Precipitation (mm) (longterm mean)				
Tuyuksu 28.0 km ² (25%)	1983	2.8 (3.6)	251 (244)	23 (17)	– 242	– 43 (– 26)	1.00 (1.02)
Ala Archa 31.0 km ² (36%)	1972	1.2 (3.6)	315 (244)	4 (17)	1	– 10 (– 5)	0.75 (1.02)
Oigaing 463 km ² (7%)	1964	3.2 (3.1)	170 (161)	71 (66)	– 296	– 68 (– 47)	1.24 (1.33)
Abramov 55.5 km ² (51%)	1972	1.6 (3.1)	177 (161)	72 (66)	– 135	– 54 (– 31)	0.95 (1.33)
Glacier No.1 3.3 km ² (55%)	1980	6.7 (5.4)	10 (44)	8 (8)	– 11	26 (13)	0.85 (0.79)
	1972	2.6 (5.4)	59 (44)	7 (8)	57	– 20 (– 11)	0.68 (0.79)
	1975	4.2 (4.2)	79 (70)	70 (66)	– 495	– 86 (– 64)	1.27 (1.18)
	1981	2.4 (4.2)	129 (70)	53 (66)	– 63	– 75 (– 57)	0.81 (1.18)
	1988	2.0 (1.8)	250 (185)	53 (39)	– 234	– 70 (– 57)	0.93 (0.81)
	1989	1.5 (1.8)	189 (185)	24 (39)	– 7	– 59 (– 50)	0.58 (0.81)

Conclusions

Satisfactory values for the goodness of fit have shown that the conceptual HBV-ETH precipitation–runoff model is capable of simulating runoff in the continental climate of Central Asia.

Runoff scenarios for a warmer climate and different steps of deglaciation display a similar general behaviour as former studies in the Alps (Hagg 2003; Hagg and Braun 2005) have revealed. Quantitative differences are mainly due to the degree of glaciation, glacier mass balance behaviour and local weather patterns in the reference period. These factors control water balances of small head watersheds and their reaction to climate changes to a higher degree than any large scale climate parameter such as continentality.

The most important features of the hydrological reaction are the increase of discharge during snowmelt with rising temperatures and the shortage of summer runoff with the disappearance of glaciers. The higher flood risk is more restricted to areas within the mountains, where the water runs off quickly in steep and narrow flow paths. The occurrence of debris flows and other mass movements is favoured by the allocation of loose material under retreating glaciers and conducted by the formation of moraine dammed lakes, which represent another hazard for the mountain population. Shortage of summer runoff will have a greater distant effect on surrounding lowlands. The greater the hydrological difference between mountains and lowland, the more the foreland depends on mountain runoff and the more significant are changes in mountain hydrology. The dry forelands of the Central Asian mountains strongly depend on glacier melt, which is a major source of water during the dry vegetation period. Agriculture is only possible with irrigation and many regions will face a serious water deficiency if the glaciers continue to shrink at rates as observed today. The consequences and problems will not only be economic, but also social, hygienic and ecological.

Acknowledgements

The work was funded by the German Research Foundation (DFG, project BR1622/5-3 and BR1622/6-1) and supported by the Bavarian Academy of Sciences. The authors thank Professor Igor Severskiy, Professor Vladimir Aizen, Dr Felix Pertziger, Professor Ersi Kang and their colleagues for providing data.

References

- Ageta, Y. and Higuchi, K. (1984). Estimation of mass balance components of a summer-accumulation type glacier in the Nepal Himalaya. *Geografiska Annaler*, **66A**(3), 249–255.
- Bergström, S. (1976). Development and application of a conceptual model for Scandinavian catchments, University of Lund Bulletin 52A.
- Braun, L.N. and Aellen, M. (1990). Modelling discharge of glacierized basins assisted by direct measurements of glacier mass balance. *IAHS Publ.*, **193**, 99–106.
- Braun, L.N. and Renner, C.B. (1992). Applications of a conceptual runoff model in different physiographic regions of Switzerland. *Hydrol. Sci. J.*, **73**(3), 217–231.
- Braun, L.N., Weber, M. and Schulz, M. (2000). Consequences of climate change for runoff from Alpine regions. *Annals Glaciol.*, **31**, 19–25.
- CADB (2003). *Central Asia Database*. Internet Datacollection of the University of Idaho (Prof. V. Aizen). Available at: <http://www.webpages.uidaho.edu/~aizen/centralasia/CADB.html>.
- Escher-Vetter, H., Weber, M. and Braun, L.N. (1999). Auswirkungen von Klimaänderungen auf den Wasserhaushalt hochalpiner, teilweise vergletscherte Gebiete. Abschlussbericht BayFORKLIM. On: “Klimaerwärmung Gletscher – wie verändern sich die Gebirgsabflüsse” CD-ROM. Kommission für Glaziologie, Bayerische Akademie der Wissenschaften, München.
- Fluctuations of Glaciers, Vol. IV (1975–1980). (1985). Haeberli, W. [Hrsg.]. IAHS (ICSU)-UNESCO, Zürich.

- Hagg, W. (2003). Auswirkungen von Gletscherschwund auf die Wasserspende hochalpiner Gebiete, Vergleich Alpen - Zentralasien. *Münchner Geographische Abhandlungen*, **53(A)**, München. Available at: <http://edoc.ub.uni-muenchen.de/view/subjects/fak20.html>.
- Hagg, W. and Braun, L.N. (2005). The influence of glacier retreat on water yield from high mountain areas: comparison of Alps and Central Asia. In: *Climate and Hydrology in Mountain Areas*, C. De Jong, R. Ranzi and D. Collins (Eds.), Wiley & Sons, Chichester, pp. 263–275.
- IPCC (2001). *Climate Change 2001 Working Group II: Impacts, Adaptation and Vulnerability*. Intergovernmental Panel on Climate Change. WMO, UNEP.
- Hennessy, R.J., Gregory, J.M. and Mitchell, J.F.B. (1997). Changes in daily precipitation under enhanced greenhouse conditions. *Climate Dyn.*, **13**, 667–680.
- KazNIIMOSK (1999). *Climate change and a new defence strategy against mudflows and snow avalanches. National Report on the Impact and Adaptation Assessment for the Mountain Region of South and Southeast Kazakhstan and the Kazakh part of the Caspian Sea Coastal Sector*. Netherlands Climate Change Studies Assistance Programme, Kazakhstan Climate Change Study vol. 1, Kazakh Research Institute For Environment Monitoring and Climate, Almaty.
- Kommission für Glaziologie (2003). Gletschergebiet Tjuksu, Sailiski Alatau. Map 1:10'000. *Fluctuations of Glaciers 1995–2000* vol. VIII, World Glacier Monitoring Service, Zürich.
- McGuffie, K., Henderson-Sellers, A., Holbrook, N., Kothavala, Z., Balachova, O. and Hoekstra, J. (1999). Assessing simulations of daily temperature and precipitation variability with global climate models for present and enhanced greenhouse climates. *Int. J. Climatol.*, **19**, 1–26.
- Nash, J.E. and Sutcliffe, J.V. (1970). River flow forecasting through conceptual models. Part I - a discussion of principles. *J. Hydrol.*, **10(3)**, 282–290.
- Rango, A. (1992). Worldwide testing of the snowmelt runoff model with applications for predicting the effects of climate change. *Nordic Hydrol.*, **23**, 155–172.
- Richardson, C.W. (1981). Stochastic simulation of daily precipitation, temperature and solar radiation. *Wat. Res. Res.*, **17**, 182–190.
- Semenov, M.A., Brooks, R.J., Barrow, E.M. and Richardson, C.W. (1998). Comparison of the WGEN and LARS-WG stochastic weather generators for diverse climates. *Climate Res.*, **10**, 95–107.
- WGMS (1999). *Glacier Mass Balance Bulletin No. 4*, IAHS (ICSU)-UNEP-UNESCO-WMO, compiled by the World Glacier Monitoring Service, Zürich.
- WGMS (2001). *Glacier Mass Balance Bulletin No. 6*, IAHS (ICSU)-UNEP-UNESCO-WMO, compiled by the World Glacier Monitoring Service, Zürich.